

Topology and \mathcal{PT} Symmetry in a Non-Hermitian Su-Schrieffer-Heeger Chain with Periodic Hopping Modulation

Surajit Mandal, Satyaki Kar*

AKPC Mahavidyalaya, Bengai, West Bengal -712611, India

We study the effect of periodic hopping modulation on a Su-Schrieffer-Heeger (SSH) chain that exhibits non-Hermiticity in presence of an onsite staggered imaginary potential. This dissipative, non-Hermitian (NH) extension amply modifies the features of the topological trivial phase (TTP) and the topological nontrivial phase (TNP) of the SSH chain. Though a weak potential can respect the parity-time (\mathcal{PT}) symmetry keeping the energy eigenvalues real, a strong potential breaks \mathcal{PT} conservation leading to imaginary end state and complex bulk state energies in the system. Furthermore for large commensurate periodicity of the hopping, in-gap states appear that take either purely real or purely imaginary eigenvalues depending on the strength of both NH potential and hopping modulation. In particular, this paper is engaged with hopping periodicities of 2, 4 and 8 lattice spacings. The localization of end states and in-gap states at the boundaries are investigated for those hopping periodicities. Though we find that topology and \mathcal{PT} symmetry are not very directly connected, distinguishing distribution of \mathcal{PT} broken and unbroken phases are clearly observed within TNP and TTP in our systems.

I. INTRODUCTION

As per the Dirac-Von Neumann's formulation in quantum mechanics, all the physical observables in the Hilbert space are represented by Hermitian operators[1], which in turn gives the real eigenvalues in the energy spectrum with the assurance the conservation of probability. Interestingly, a wide class of non-Hermitian Hamiltonians that respect \mathcal{PT} -symmetry can also display entirely real energy eigenvalues[2] thereby garnering huge attention nowadays from the Physics community.

There is a fundamental difference between the \mathcal{PT} transitions and transitions in normal topological insulators. For example, in the Hermitian SSH chain, end modes appear in TNP with nonzero winding number until the band gap closes at quantum phase transition (QPT). But in an NH extension of this model, the bulk band crossings are visible (in the imaginary energy axis) throughout the entire \mathcal{PT} -broken phase[3] even in presence of the end modes as long as the model belongs to TNP. Whenever the bulk modes start getting complex eigenvalues (*i.e.*, no more remaining purely real) the \mathcal{PT} transition takes place in the NH model, be it either within TNP or TTP. In fact, one gets a \mathcal{PT} broken phase positioned symmetrically about the QPT (having zero dimerization parameter Δ) within a parameter range proportional to the NH potential strength. The global invariant such as pseudo-anti-Hermiticity of \mathcal{PT} -symmetric model turns the end modes gapless in the real energy plane while gapped in the imaginary plane. This relies on the fact that bulk band crossings occur far from the topological transition point implying the invariant to be a property of the entire Hamiltonian instead of individual bands[3]. In the case of open boundary conditions (OBC), the TNP of the SSH model shows topologically protected mid-gap states while the end modes of the non-Hermitian SSH model have complex energy eigenvalues rather than zero energy eigenvalues[3–6]. As per the well-

known Non-Hermitian skin effect, the bulk states in addition to topological end states become localized near the edges for nonreciprocal lattices[7].

The intricate interplay between the topological properties and the spontaneously \mathcal{PT} breaking transition (SPT BT) has been studied previously by Wang *et. al.*[4]. They found that there is no such direct correlation of the same. In this work, we aim to seek this correlation in the presence of periodically modulated hopping amplitude in the SSH chain which will facilitate further understanding of the issue.

Klett *et. al.*, have shown that the SSH model under the consideration of an imaginary staggered onsite potential shows a SPT BT in the TNP[5]. Under the same staggered potential, our system of concern, for all commensurate θ values, undergoes a SPT BT at an exceptional point (EP) in the TNP and when modulation parameter Δ is near the transition point/phase boundary. In addition, our system of interest lies in a spontaneous \mathcal{PT} broken phases (SPT BP) for all nonzero arbitrary values of γ with Δ deep within the TNP far away from the transition point. In TTP, however, SPT BP appears when the bulk modes become complex in energy. The appearance of SPT BP in the TNP for our system is similar to another NH extension of the SSH model involving only imaginary boundary potentials[6].

This paper gives a detailed account of how the bulk, end modes as well as in gap modes in the periodically hopping modulated chain behave in presence of the imaginary staggered onsite potential and thus provides important feedback in utilizing them in the field of topological quantum computation.

II. \mathcal{PT} -SYMMETRIC MODEL

One dimensional Hamiltonian for non-Hermitian SSH model with staggered nearest-neighbor hopping and on-

site imaginary potentials becomes

$$\mathcal{H}_{\mathcal{PT}} = \mathcal{H}_{SSH} + U, \quad (1)$$

in which \mathcal{H}_{SSH} is the Hamiltonian of SSH chain of $L = M * N$ (M and N are the number sublattice and unit cells respectively) sites with modulated hopping strength and defined as

$$\mathcal{H}_{SSH} = \sum_i^{L-1} (t + \delta_i) [|i\rangle \langle i+1| + H.c], \quad (2)$$

where $\delta_i = \Delta \cos[(i-1)\theta]$ with $i = 1, 2, 3, \dots, n$ gives the periodic modulation in hopping strength (t). Generally, one acquire $\delta_{i+1} = \Delta \cos(\frac{2\pi i}{M})$ when $\theta = \frac{2\pi}{M}$ and the chain shows a M sublattice structure. One can represent the system by a $M \times M$ Hamiltonian matrix having M number of eigenmodes. The onsite term U is \mathcal{PT} -symmetric and is given by

$$U = i\gamma \sum_i^L (-1)^{i-1} |i\rangle \langle i|, \quad (3)$$

in which the coefficient $\gamma > 0$ is called the gain-loss contrast as it indicates the gain or loss of particles in this dissipative 1D system. Notice that Eq.2 is chiral symmetric while Eq.1 is not. However, Eq.1 is \mathcal{PT} symmetric. Though the parity/space-inversion (\mathcal{P}) and time-reversal (\mathcal{T}) operator individually does not commute with $H_{\mathcal{PT}}$, the Hamiltonian remains invariant under the combined effect of parity and time-reversal, $[\mathcal{PT}, \mathcal{H}_{\mathcal{PT}}] = 0$ (with

$\hat{\mathcal{PT}}$ is the \mathcal{PT} symmetry operator) which helps the complex energy eigenvalues to become entirely real in the \mathcal{PT} -symmetric eigenstates. However, there are parameter regime where the Hamiltonian symmetry is broken spontaneously in some/all eigenstates thereby producing complex eigenvalues[9].

It is obvious that chiral or sublattice symmetry which protects the end states in a SSH model can be given by the operator $\tau_z = \mathbb{I}_N \otimes \sigma_z$ with \mathbb{I}_N referring to the $N \times N$ identity matrix[11]. Hence the SSH Hamiltonian follows the anticommutation: $\{\mathcal{H}_{SSH}, \tau_z\} = 0$. However, this no longer holds good for the non-Hermitian model Hamiltonian Eq.1 in the presence of a staggered imaginary potential: $\gamma \neq 0$ [3] and the underlying symmetry relation needs to be modified for non-Hermitian systems[10]. From an analogy of the Hermitian case, here one can think of a many body symmetry operator $\Lambda = \tau_z \mathcal{T}$, in which \mathcal{T} denotes the complex conjugation (for this spin-polarized/spinless case) representing the time-reversal operator[9, 11]. Like the chiral operator of the Hermitian case, here also the newly defined non-Hermitian operator Λ satisfy $\Lambda^\dagger \mathcal{H}_{\mathcal{PT}} \Lambda = -\mathcal{H}_{\mathcal{PT}}$ which led to the “pseudo-anti-hermiticity” property[9]. This makes the spectrum symmetric about both the real and imaginary axis and one can have a quartet of \mathcal{PT} symmetric states with energies $E, -E, E^*$ and $-E^*$ [2, 11–14].

As per the symmetry of the eigenfunctions[2], the NH system can possess a broken or an unbroken \mathcal{PT} -symmetry. Recalling the time-independent Schrödinger equation of eigenvectors $|\psi\rangle$ as

$$\mathcal{H}_{\mathcal{PT}} |\psi\rangle = E |\psi\rangle, \quad (4)$$

θ values	QPT point	TNP	TTP
π	$\Delta/t = 0$	$\Delta/t < 0$	$\Delta/t > 0$
$\pi/2$	$ \Delta/t = \sqrt{2}$	$0 < \Delta/t < \sqrt{2}$	$ \Delta/t > \sqrt{2}$
$\pi/4$	$ \Delta/t = \sqrt{2(2 \pm \sqrt{2})}$	$0 < \Delta/t < \sqrt{2(2 - \sqrt{2})}; \Delta/t > \sqrt{2(2 + \sqrt{2})}$	$\sqrt{2(2 - \sqrt{2})} < \Delta/t < \sqrt{2(2 + \sqrt{2})}$

TABLE I. QPT point, domain of the TNP and TTP of periodic modulated SSH chain for different θ values. This range of TNP and TTP is based on an earlier study as found in Ref.[15].

where E is the eigenvalues. The system should acquire real eigenvalues and respect \mathcal{PT} -symmetry if all the eigenvectors follow \mathcal{PT} -symmetry relation $\mathcal{PT} |\psi\rangle = |\psi\rangle$. However, the system generates broken \mathcal{PT} -symmetry if all the eigenfunctions do not obey this relation, and the corresponding eigenvalues are complex[6].

In the absence of imaginary potential Eq.(3), Eq.(1) re-

duces to a hopping modulated Hermitian SSH chain[15]. For $\theta = \pi$, this chain shows a two-band spectrum. The quantum phase transition point (QPT) within the band spectra is important in finding the topological domain and such domain for various commensurate θ values for the isolated/Hermitian (when $\gamma = 0$) SSH chain is given in Table I. The zero energy states (ZES) found in the do-

main of TNP for an isolated SSH chain (as mentioned in Table.I) are protected by particle-hole as well as inversion symmetry[16]. In the following section, we mainly focused on the TNP and TTP for all the commensurate θ values to see their exotic behavior in the presence of an alternating gain and loss strength γ in terms of an onsite imaginary potential. Importantly, the QPT point of the Hermitian system is now called as \mathcal{PT} symmetric transition point[3]. The transition point is a crossover after that the system enters into a completely \mathcal{PT} -symmetry broken region.

III. NUMERICAL RESULT

This section is devoted to accumulating the numerical calculations of eigenvalue Eq.(4) of the above mentioned models under the consideration of OBC. We delve into investigating the effects of alternating gain and loss on the topological/trivial regime of the energy spectrum for the concerned system.

A. Case of $\theta = \pi$

The considered model, for this θ value, is staggered by modulation parameter $\pm\Delta$ which in turn fully corroborates the usual SSH chain. In bulk momentum (k) space, the model Eq.(1) gives the single-particle Bloch Hamiltonian for $\theta = \pi$ as:

$$\mathcal{H}_{\mathcal{PT}}(k) = \begin{pmatrix} i\gamma & A_k \\ A_{-k} & -i\gamma \end{pmatrix}, \quad (5)$$

where, $A_k = (t + \Delta) + (t - \Delta)e^{-ik}$. It turns out to be the Bloch Hamiltonian of Hermitian system in the limit $\gamma \rightarrow 0$. It can be written using Pauli matrices σ_i as

$$\mathcal{H}_{\mathcal{PT}}(k) = [(t+\Delta) + (t-\Delta)\cos(k)]\sigma_x + (t-\Delta)\sin(k)\sigma_y + i\gamma\sigma_z \quad (6)$$

and dispersion relation obtained as

$$E(k)_{\pm} = \pm\sqrt{2}\sqrt{t^2 + \Delta^2 + (t^2 - \Delta^2)\cos k} - \gamma^2 \quad (7)$$

in which k is the single-particle momentum. Thus for a periodic system, a larger γ results in narrower band gap for fixed Δ/t . For small Δ/t , all eigenvalues becomes real for all the Bloch states as long as $\gamma < 2|\Delta|$ making the system \mathcal{PT} symmetric[17, 18] (see Fig.1(d)-(e), for example) while for $\gamma > 2|t|$ one gets imaginary eigenvalues for all k values (see Fig.1(f)) giving a completely \mathcal{PT} -symmetry broken phase. Moreover, the system goes into a partially \mathcal{PT} broken region whenever $2|t| > \gamma > 2|\Delta|$ [11] where the energy eigenvalues become real for some values of k and imaginary for the other. For an open (finite) system, however, there are end states in the TNP region and the corresponding eigenvalue go from real to imaginary at a much smaller critical value of

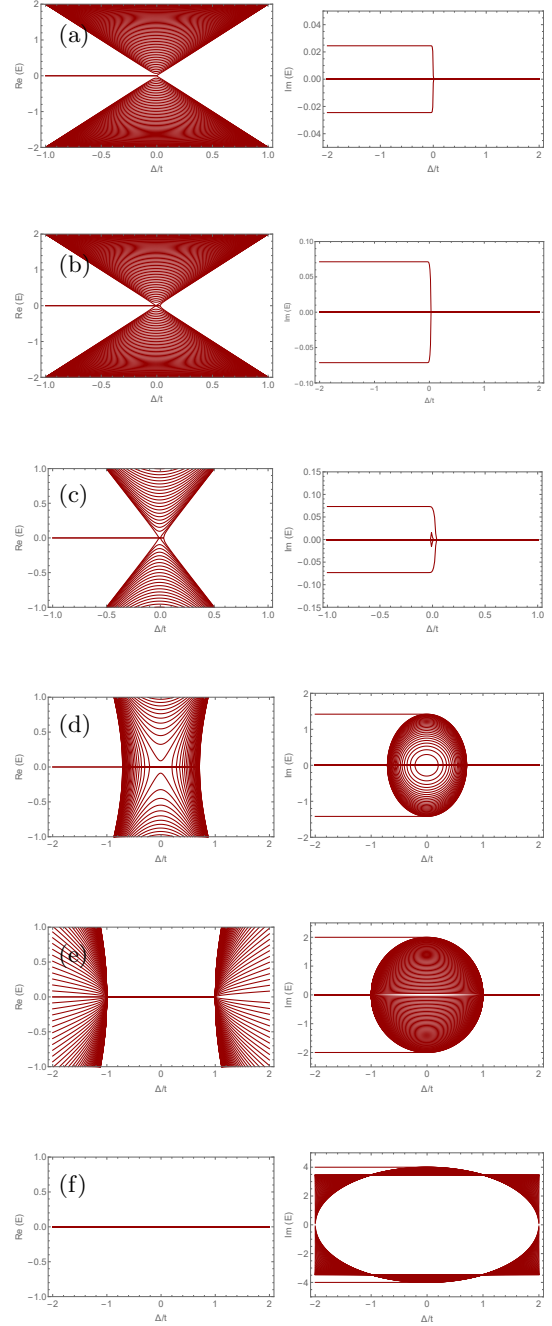


FIG. 1. Numerical spectra (**real**(left) and the **imaginary** (right) part of the eigenvalue) of an **open chain** for the \mathcal{PT} -symmetric non-Hermitian SSH model with respect to Δ/t ($\in [-2, 2]$) with $t = 1$, $L = 128$ and for $\gamma =$ (a) 2.45×10^{-2} , (b) 7.136×10^{-2} , (c) 7.32×10^{-2} , (d) 1.42, (e) 2 and (f) 4 respectively.

γ_{ep} ($\ll 2|\Delta|$) called an exceptional point (EP)[11]. It is worthwhile to mention that one can estimate the winding number (considering the same form as in the Hermitian case[14]) for the periodic system when the bulk band gap appears[20]. Hence $\mathcal{W} \neq 0$ for nontrivial topological cases when $\frac{t-\Delta}{t+\Delta} > 1$ and $\gamma < 2|\Delta|$ (open gap)[11]. The

energy spectra under OBC in the TNP ($\Delta/t < 0$) and the TTP ($\Delta/t > 0$) regimes show features different from the conventional SSH chain in the presence of an onsite imaginary potential U and are presented in Fig.1.

Firstly, we proceed to discuss how the properties of the TNP get changed with γ . Notice that the real spectra for small $\gamma = 2.45 \times 10^{-2}$ depicted in Fig.1(a) has identical behavior to that of the usual SSH model[15] and here two (purely)real bulk bands are separated by midgap zero modes which however possess imaginary eigenvalues. For higher γ , few bulk bands with small real energy start getting its imaginary components gradually (see Fig.1(c)-(f))[3]. Moreover, the mid-gap states (here, we call them ZES) having $Re[E] = 0$ and conjugated imaginary energies $\pm i\beta$ (where β should depend on Δ/t and γ) indicate end state behavior[3, 6] throughout the TNP (*i.e.*, $\Delta/t < 0$). /in that sense they can be called gapped end states. The \mathcal{PT} phase diagram Fig.2(a) shows the variation of eigenvalues of the end states with γ indicating appearance of complex conjugate pair of eigenvalues in TNP beyond $\gamma = \gamma_{ep}$ resulting in a \mathcal{PT} symmetry breaking in the TNP for $\gamma \geq \gamma_{ep}$. In contrast, a purely real spectrum is observed in the Kiteav chain as they obey particle-hole symmetry and lead to the \mathcal{PT} symmetric end state[3]. This indicates that, as γ is introduced and gradually increased in the system, it is the symmetry of the end states that provides the overall \mathcal{PT} -symmetry rather than the mere existence of TNP, as also elaborated in Ref.[5]. The broken \mathcal{PT} -symmetry of the end modes for small γ ($> \gamma_{ep}$ though) is again responsible for destroying the stability of zero-modes of a periodically modulated SSH model in the TNP[6]. For the particular value of γ as mentioned above, there are only two conjugated eigenvalues corresponding to a gapped end state (as discussed above) in the imaginary spectrum and the remaining $2N - 2$ eigenvalues are purely real. Notice that unlike our chiral symmetry broken system, the end modes in the models respecting chiral symmetry are gapless with zero energies[3]. Then for $\gamma = 7.32 \times 10^{-2}$ in Fig.1(c), few of the gapped bulk modes also get nonzero imaginary component in energy for γ close to the **topological transition point** (compare with the range of $2|\Delta| < \gamma$ for periodic chain), similar to another \mathcal{PT} -symmetric model studied in Ref.[3]. Notice that such transition for very small γ is not discernible well as it falls very close to the QPT. The gap between the the end state pairs entirely depends on γ as $E_{edge} = \pm i\gamma$ with gap increasing linearly with γ [see right panels of Fig.1]. Even for the bulk modes whose energy become complex (beginning from situation like in fig.1(c)), the energy gap in the imaginary plane also increases with γ . Interestingly all the bulk energy modes become purely imaginary for $|\Delta| < \Delta_0$ at a critical value: $\gamma_c \simeq 1.9$ for $\Delta_0/t = 1$ as well as higher γ values with larger Δ_0 (see Fig.1(e),(f) and compare with the limit of $\gamma > 2t$ in the periodic chain). Notice that for $\gamma > \gamma_c$, ZES survives when $\Delta < -\Delta_0$ while it occurs for $\Delta/t < 0$ otherwise[14]. One end state appears at the left boundary while the other at the right boundary [see

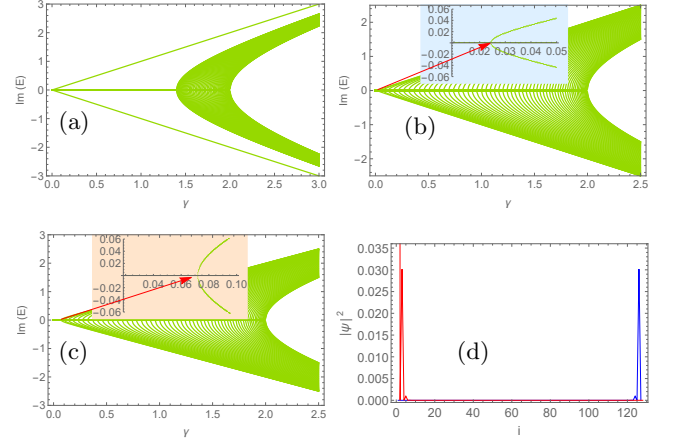


FIG. 2. Numerical spectra of the **imaginary part** of the eigenvalue against γ with $t = 1$, $L = 128$ and $\Delta/t =$ (a) -7×10^{-1} (system in the TNP), (b) 0 (system at the phase boundary) and (c) 3.01×10^{-2} (system in the TTP). The amplitude distribution of two complex end states in the TNP is shown in (d). Inset represents the exact location of *SPT BT* point.

Fig.2(d)]. The properties of non-Hermitian end states in summarized in Table.II.

Now, we study the TTP which is prominent in the domain of $\Delta/t > 0$. One can notice only gapped bulk modes with entirely real energy eigenvalues for $\gamma = 2.45 \times 10^{-2}$ [see Fig.1(a)], retaining the \mathcal{PT} -symmetry there. However, the TTP in contrast to the TNP doesn't support any gapped end mode. But other than that, the spectra is symmetric with respect to the sign of Δ/t , even in presence of γ . Even though the TTP preserves \mathcal{PT} -symmetry for small γ , they lose the same for larger values of it [see Fig.2(b)]. Particularly Fig.2(b) depicts that the imaginary eigenvalues start to appear at the phase boundary of $\Delta/t \rightarrow 0$ [22] at $\gamma = 2.45 \times 10^{-2}$.

As we studied above, the nonzero γ values results in one *SPT BP* in the TNP as shown in Fig.2(a), though followed by a *SPT BT* for a weak value of γ where the end state eigenvalues collapse to zero[11]. Though γ_{ep} goes to zero for infinite chain limit, for a finite chain it depends on Δ like that shown in Fig.3(a). One can already notice that the symmetry breaking of our considered model depends not only on γ but also on Δ/t values (for $\gamma \neq 0$) because Δ/t determines the domain of the topological phases in the parameter space. Notice that near the \mathcal{PT} transition point[23] within TNP, the model shows entirely real (imaginary) end-state spectra leading to \mathcal{PT} unbroken (broken) phase with γ smaller (larger) than γ_{ep} [see Fig.3(b)]. Consequently, *SPT BT* occurs at the γ_{ep} of this system. For particular consideration of $\Delta/t = -2.5 \times 10^{-2}$, the value of γ_{ep} for this case can be estimated by the diagonalization the Eq.(1) and comes out to be $\gamma_{ep} = 3.98 \times 10^{-3}$.

The above value of \mathcal{PT} -symmetry breaking point, γ_{ep} is verified by the analytical expression proposed in Ref.[11]. The plot of end states display that they have an equal share on both ends for $\gamma < \gamma_{ep}$ [Fig.3(c)] while for

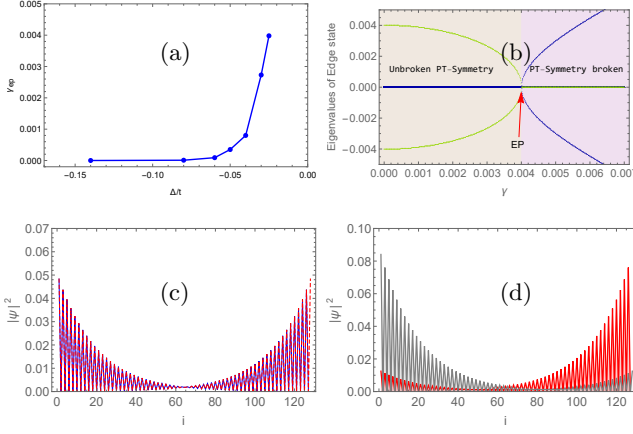


FIG. 3. (a) Variation of γ_{ep} with Δ (b) γ_{ep} for our model under the TNP configuration with $\theta = \pi$. The behavior of end states at lattice site i (absolute values of amplitudes) for smaller (c) and greater (d) than γ_{ep} . The chosen parameters are $L = 128$ and $\Delta/t = -2.5 \times 10^{-2}$ (very close to the transition point).

$\gamma > \gamma_{ep}$, non-Hermitian end states emerge[14, 21, 24, 25] where the eigenvalues become imaginary. Here, the left non-Hermitian end state tilts towards the right end and vice-versa [see Fig.3(d)]. The bulk states don't show localization rather they display the extended nature and our model not being non-reciprocal, the non-Hermitian skin effect[26, 31] is not found here. We can, however, add here that under strong dimerization (*i.e.*, $\Delta \sim t$), these NH model can exhibit simple harmonic dynamics at EP[27].

1. Winding Number

Now we generalize the ZAK phases generalized for these dissipative cases.[9] The topological number for the

considered model is the winding number[14]

$$\mathcal{W} = \frac{1}{2\pi i} \int_0^{2\pi} q(k)^{-1} \partial_k q(k) dk \quad (8)$$

where the complex function $q(k)$ is the upper off-diagonal block of the matrix $Q(k)$ [14, 28] and defined as

$$Q(k) = \begin{pmatrix} 0 & q(k) \\ q(k)^* & 0 \end{pmatrix}, \quad (9)$$

However, $Q(k)$ is defined from the non-Hermitian generalizations of projection operators via $Q(k) = Q'(k) + Q'(k)^\dagger$ with $Q'(k) = \frac{1}{2} \left(\sum_{n>0} |\psi_n(k)\rangle \langle \psi_n(k)| - \sum_{n<0} |\psi_n(k)\rangle \langle \psi_n(k)| \right)$ in which $|\psi_n(k)\rangle$ and $\langle \psi_n(k)|$ are the left and right eigenstates of $\mathcal{H}_{\mathcal{PT}}(k)$. Using Cauchy residue theorem, we can arrive at $\mathcal{W} = 1(0)$ for $\Delta/t < 0(> 0)$. As per bulk-energy correspondence, the nonzero winding number predicts ZES (in the real part of energy eigenvalues) on the boundary[29] and in our system this occurs for $\Delta/t < 0$. More precisely, the end state with energy $Re[E] = 0$ is estimated in the region of $\Delta/t < 0$ provided that $\gamma < 2|\Delta|$ such that bulk energy gap remains open.

B. Case of $\theta = \pi/2$

Let us now study the properties of nontrivial and trivial phases for this case when non-Hermiticity is induced by switching on the parameter γ . In order to do this, we first write the Hamiltonian in the k -space and becomes

$$\mathcal{H}_{\mathcal{PT}}(k) = \begin{pmatrix} i\gamma & (t + \Delta) & 0 & te^{-4ik} \\ (t + \Delta) & -i\gamma & t & 0 \\ 0 & t & i\gamma & (t - \Delta) \\ te^{4ik} & 0 & (t - \Delta) & -i\gamma \end{pmatrix}, \quad (10)$$

with energy eigenvalues

$$E(k) = \pm \sqrt{2t^2 + \Delta^2 - \gamma^2 \pm t \sqrt{2t^2 + 6\Delta^2 + 2(t^2 - \Delta^2) \cos 4k}}. \quad (11)$$

The above dispersion relation gives the \mathcal{PT} classification of the bulk modes. For $|\Delta/t| < (>) 1$, let's define parameters γ_1 and γ_2 as $2t^2 + \Delta^2 - \gamma_1^2 = 2t\sqrt{t^2 + \Delta^2}(2t\sqrt{2\Delta^2})$ and $\gamma_2^2 = 2t^2 + \Delta^2 + 2t\sqrt{t^2 + \Delta^2}(2t\sqrt{2\Delta^2})$. Then all the bulk modes become real when $\gamma < |\gamma_1|$ and bulk states show entirely imaginary eigenvalues for $\gamma > |\gamma_2|$. We can notice that the gain and loss strength make the efficient modulation of the band gaps for the real and imaginary parts of the energy eigenvalues. First, we discuss the TNP regime,

i.e., the regime of $0 < |\Delta/t| < \sqrt{2}$ (see Table.I). The variation of the real and imaginary part of energy with Δ/t under OBC for different values of γ is shown in Fig.4. Similar to the situation of $\theta = \pi$, here for small γ ($= 5 \times 10^{-3}$) values, the TNP consists of a pair of purely imaginary gapped end states along with purely real bulk modes [Fig.4(a)]. In order to get a bit clearer vision, one can look at the \mathcal{PT} phase diagram[5] presented in Fig.5(a) which shows that topological end states with imaginary eigenvalues begin to emerge soon after γ is in-

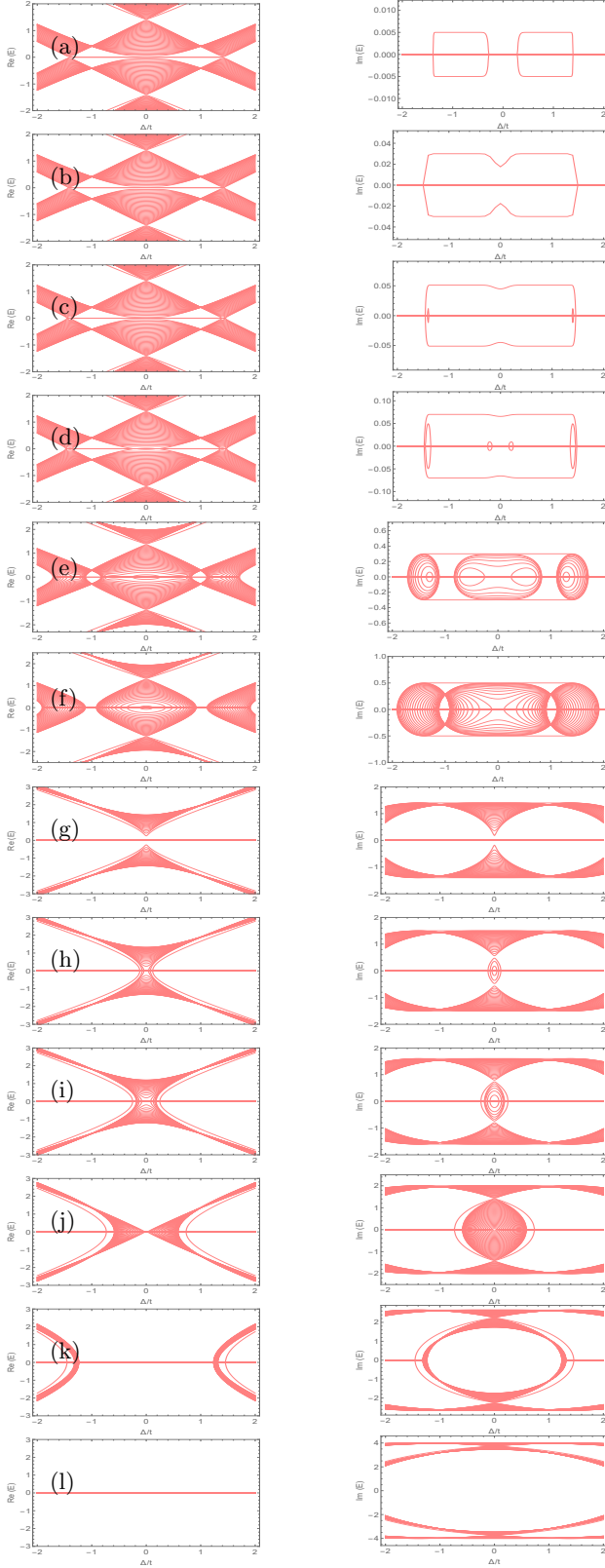


FIG. 4. Numerical spectra of the **real** (left) and **imaginary** (right) part of the energy eigenvalues of an **open chain** for the \mathcal{PT} -symmetric non-Hermitian SSH model with $\Delta/t \in [-2, 2]$ with $t = 1$, $L = 128$ and for various $\gamma =$ (a) 5×10^{-3} ; (b) 3×10^{-2} ; (c) 5.1×10^{-2} ; (d) 7×10^{-2} ; (e) 3×10^{-1} ; (f) 5×10^{-1} ; (g) 1.4; (h) 1.5; (i) 1.6; (j) 2; (k) 2.652; (l) 4.

creased from a zero value. We also notice that the eigenvalues near $\Delta/t \rightarrow 0$ remain purely real. However, this region breaks \mathcal{PT} -symmetry for larger γ ($\sim 3 \times 10^{-2}$) values with the presence of end states with imaginary energy even at $\Delta = 0$ [Fig.4(b)]. The bulk states are real until $\gamma = 5.1 \times 10^{-2}$ when complex-valued gapped bulk modes start appearing at the transition point $|\Delta/t| = \sqrt{2}$ [Fig.4(c)]. With further increase in γ say at $\gamma = 7 \times 10^{-2}$ [Fig.4(d)], more complex bulk modes appear in the vicinity of $|\Delta/t| \rightarrow 0$. Unlike the $\theta = \pi$ case, this case admits 2 new in-gap states [15] which shows only real eigenvalues in the energy spectrum for $0 < \gamma \lesssim 1.4$ [Fig.4(a)-(g)]. Interestingly, the in-gap modes start acquiring imaginary eigenvalues when $\gamma = 1.5$ at $|\Delta| \leq 1.2 \times 10^{-1}$ (Fig.4(h)) or at $|\Delta/t| \leq 2.5 \times 10^{-1}$ for $\gamma = 1.6$ [Figs.4(i)]. For $\gamma = 2$ [see Fig.4(j)] the bulk modes gain purely imaginary eigenvalues near $\Delta/t \rightarrow 0$, while the imaginary conjugated in-gap pairs for this particular situation can be found at $|\Delta/t| \leq 7.32 \times 10^{-1}$ [Fig.4(j)]. We find that from this critical value $\gamma_c = 2$ onwards, an increasing γ results in further stretched ranges of $|\Delta|$ for which purely imaginary bulk modes as well as in-gap modes are obtained. Fixing Δ/t value at 7.32×10^{-1} , how the imaginary spectrum of the bulk states, in-gap pairs or end-state pairs changes with γ can be noticed from Fig.5(a). For $\gamma > 2$, the bulk modes have purely imaginary eigenvalues in the form of $\pm i\beta$ which lasts for larger ranges of Δ/t that incidentally covers whole TNP [for $\gamma \sim 2.825$] and beyond [Fig.4(l)]. The bulk states for weak γ [Fig.4(a)-(d)] doesn't support any imaginary eigenvalue except at the gap-closing points. For intermediate values of γ , one gets complex bulk mode eigenvalues [Fig.4(e)-(i)] While for large γ , the bulk states hold purely imaginary eigenvalues [Fig.4(j)-(l)].

Now we turn to the TTP region i.e., the regime of $|\Delta/t| > \sqrt{2}$. Again, real bulk bands are found for smaller γ values. With larger γ , for example for $\gamma \gtrsim 5.0 \times 10^{-2}$ [Fig.4(c)], both TNP and TTP close to the transition point features the bulk modes with conjugated imaginary eigenvalues. Within TTP, the energy spectra is entirely real below such critical γ turning this into a \mathcal{SPT} \mathcal{BT} point. Furthermore, the energy of the in-gap states within TTP become imaginary starting from the transition point as γ is increased beyond $\gamma = 2.652$ [see Fig.4(k)]. One can notice such behavior in the energy spectrum plot of Fig.5(d) corresponding to $\Delta/t = 1.456$. For $\gamma \gtrsim 2$, one can also observe that a larger γ pushes the critical $|\Delta|$ to higher values above which nonzero real component of the bulk modes are obtained within TTP. Interestingly, a non-Hermitian SSH model with imaginary potentials only at the boundaries can result in bifurcation of the imaginary eigenvalues for large γ values [6].

Nevertheless, very close to phase transition in a part of the TNP shows a \mathcal{SPT} \mathcal{BT} (\mathcal{SPT} \mathcal{BP}) at (followed by) the \mathcal{PT} symmetry breaking point as long $\gamma = (>) 2.7 \times 10^{-3}$ rather than considering arbitrary value [Fig.5(b)]. Thus γ_{ep} becomes 2.7×10^{-3} . Though $\Delta/t = 0$ is not Lifshitz QPT point for the Hermitian system [15], one

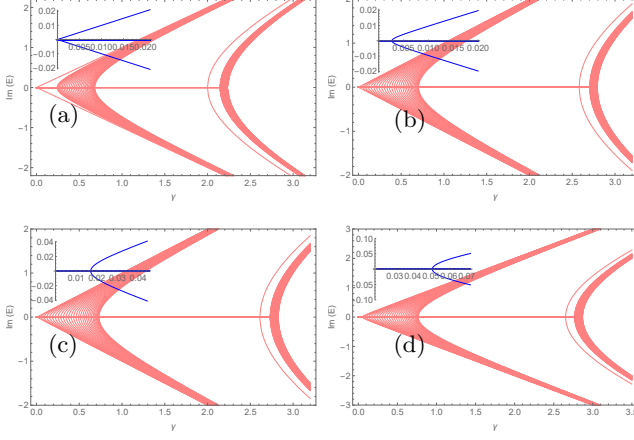


FIG. 5. Numerical spectra of the **imaginary part** of the eigenvalue under **OBC** with respect to γ with $t = 1$, $L = 128$ and $\Delta/t =$ (a) 7.32×10^{-1} (system in the TNP), (b) 1.38 (close to phase boundary), (c) 1.414 (at phase boundary) and (d) 1.456 (system in the TTP). The inset shows the appropriate position of \mathcal{SPT} \mathcal{BT} point.

C. Case of $\theta = \pi/4$

One obtains a 8×8 Bloch Hamiltonian $H_{\mathcal{PT}}(k)$ as

$$H_{\mathcal{PT}}(k) = \begin{pmatrix} i\gamma & (t + \Delta) & 0 & 0 & 0 & 0 & 0 & (t + \frac{\Delta}{\sqrt{2}})e^{-8ik} \\ (t + \Delta) & -i\gamma & (t + \frac{\Delta}{\sqrt{2}}) & 0 & 0 & 0 & 0 & 0 \\ 0 & (t + \frac{\Delta}{\sqrt{2}}) & i\gamma & t & 0 & 0 & 0 & 0 \\ 0 & 0 & t & -i\gamma & (t - \frac{\Delta}{\sqrt{2}}) & 0 & 0 & 0 \\ 0 & 0 & 0 & (t - \frac{\Delta}{\sqrt{2}}) & i\gamma & (t - \Delta) & 0 & 0 \\ 0 & 0 & 0 & 0 & (t - \Delta) & -i\gamma & (t - \frac{\Delta}{\sqrt{2}}) & 0 \\ 0 & 0 & 0 & 0 & 0 & (t - \frac{\Delta}{\sqrt{2}}) & i\gamma & t \\ (t + \frac{\Delta}{\sqrt{2}})e^{8ik} & 0 & 0 & 0 & 0 & 0 & t & -i\gamma \end{pmatrix} \quad (12)$$

The real and imaginary part of the energy eigenvalues with Δ/t for this case is presented in Fig. 6. Spectral features are similar to the previous two θ values considered in many aspects. Topological end states can also be visualized from the \mathcal{PT} phase diagram [Fig. 7]. The region of $\Delta/t \rightarrow 0$ no longer remains \mathcal{PT} -symmetric when $\gamma > 2 \times 10^{-2}$. One can notice the imaginary bulk modes to appear near the transition points of $|\Delta/t| = \sqrt{2(2 - \sqrt{2})}$ for $\gamma = 2 \times 10^{-2}$ or of $|\Delta/t| = \sqrt{2(2 + \sqrt{2})}$ for $\gamma = 9 \times 10^{-2}$ [see Fig. 6(c),(e)]. This case includes six new in-gap states that illustrate entirely real eigenvalues when $0 < \gamma \lesssim 9 \times 10^{-2}$. For critical $\gamma = \gamma_c = 2$, the eigenvalues of bulk states become purely imaginary in the vicinity of $\Delta/t \rightarrow 0$ while the in-gap states become imaginary at $\Delta/t \lesssim 3.5 \times 10^{-1}$. However, a larger $\gamma > 2$ drives a large region about $\Delta/t \rightarrow 0$ to become purely imaginary. In Figs. 6(f), two (among six) in-gap modes become complex within TNP, specifically near the phase boundary $\Delta/t = \sqrt{2(2 + \sqrt{2})}$, for $\gamma = 7.97 \times 10^{-1}$.

Within TTP, one can notice only the existence of real

can visualize the occurrence of \mathcal{PT} phase transition near $\Delta/t = 0$ in the same fashion as found in the vicinity of the transition point. Moreover, Fig. 5(c) depicts that imaginary eigenvalues begin to emerge at the transition point at $\gamma = 1.7 \times 10^{-1}$.

bulk modes when γ is weak i.e., $\gamma = 1 \times 10^{-3}$. For $\gamma \gtrsim 2 \times 10^{-2}$ [Fig. 6(b)], complex eigenvalues of the bulk start to emerge gradually growing around the phase boundary of $|\Delta/t| = \sqrt{2(2 - \sqrt{2})} \simeq 1.082$. On the other hand, complex eigenvalues appear near the other transition points of $|\Delta/t| = \sqrt{2(2 + \sqrt{2})} \simeq 2.613$ for $\gamma \gtrsim 9 \times 10^{-2}$ [Fig. 6(e)]. Thus, one obtains two critical values of $\gamma_{c1} \sim 2 \times 10^{-2}$ and $\gamma_{c2} \sim 9 \times 10^{-2}$. For instance, the imaginary spectrum against γ with $\Delta/t = 2.387$ is plotted in Fig. 7(d) to see the changes in the spectrum with γ . It can be seen from the plot that the spectrum has purely real eigenvalues when γ_{c2} and beyond this the system enters into \mathcal{SPT} \mathcal{BP} . More interestingly, here three complex pair of in-gap modes start appearing at the same $|\Delta/t|$ ($= 2.387$) but for three typical values of γ as 7.6×10^{-1} , 9.25×10^{-1} , 4.37. [see Fig. 6(g),(i),(k)]. How these different values of γ can result in the emergence of complex pairs in the spectrum for in-gap states is depicted in the \mathcal{PT} phase diagram as shown in Fig. 7(d). Additionally, Fig. 7(a),(b) displays the similar trend of oc-

curing the $SPT\ BT$ and $SPT\ BP$ in the TNP. We find the complex eigenvalues would emerge at $\gamma = 2.2 \times 10^{-2}$ at the transition point $\Delta/t = \sqrt{2(2 + \sqrt{2})}$ [Fig.7(c)].

The above analysis for all commensurate θ values indicates that the periodic modulated SSH system undergoes a $SPT\ BT$ in the TNP at a critical γ_{ep} (known as EP) close to a topological transition point while deep within the TNP, the system depicts only one $SPT\ BP$ for any arbitrary nonzero values. In this regard, there exist only real eigenvalues in the TTP for some $\gamma < \gamma_c$ above which all bulk state eigenvalues become complex leading to the occurrence of $SPT\ BP$.

1. Properties of Complex End, In-Gap and Bulk States for $\theta = \pi/2, \pi/4$

We found two ZES and two in-gap states in the topological sector (TNP) for the Hermitian case for $\theta = \pi/2$ [15] whereas, the topological sector of the non-Hermitian system consists of two complex pairs. One pair of gapped end states with energy in the form $\pm i\beta$ (but have energy $Re[E] = 0$ in a real plane) correspond to ZES while the other pair with $Re[E] \neq 0$ arises for the in-gap states [see Fig.5(a) and Fig.8(a)]. The eigenstates of the end states with $Re[E] = 0$ are not always independent of each other but in-gap states with $Re[E] \neq 0$ are independent because of their different energies[14].

Here for $\theta = \pi/2$, the amplitude distribution of the pair of end states, above γ_{ep} and deep within the TNP, shows features of localization at the single end (one at left and the other at right) of the chain [Fig.8(c)] while below γ_{ep} and close to \mathcal{PT} transition point make the complex end states to survives at both the boundaries provided that they have an equal contribution from both ends, similar to the Hermitian counterparts[11, 15]. However, we found that in-gap states related pair appearing at $\gamma = 2$ have a nonzero amplitude which shows a peak near the left end of the chain [see Fig.8(b)]. In addition, the two in-gap states in the TTP of the Hermitian case can hold complex energy eigenvalues as soon as imaginary potential U is taken into account. Interestingly, the presence of this potential can lead to intriguing results in the TTP i.e., one complex pair is likely to be found in $SPT\ BP$ at $\gamma = 2.652$ [see Fig.5(d) and 8(d)] and also peaked at the left end of the chain [see Fig.8(e)]. How the properties of ZES and in-gap states of the Hermitian system get affected in the TNP and TTP for the consideration of γ is summarized in Table.III.

However, even though all the bulk states have complex eigenvalues they elucidate *extended profiles* throughout the lattice [see Fig.8(f)]. Thus, two complex pairs in the TNP and one pair in TTP don't illustrate the non-Hermitian skin effect[26, 31]. One can observe similar trends for $\theta = \pi/4$ as illustrated in Fig.9 and can have a look at Table.III for the properties of complex topological end and in-gap states. Further consideration of asymmetric hopping strength in forward and backward

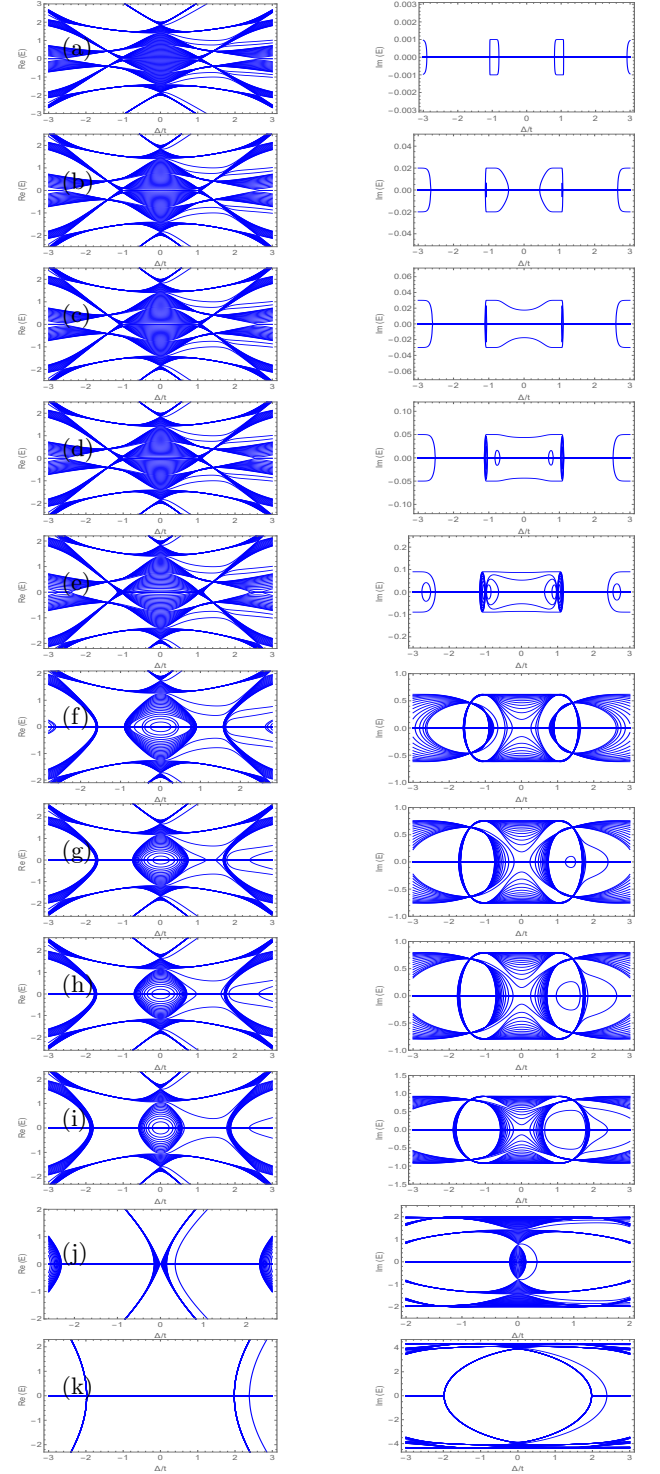


FIG. 6. Numerical spectra of the **real** (left) and **imaginary** (right) part of the energy eigenvalues of an **open chain** for the \mathcal{PT} -symmetric non-Hermitian SSH model with $\Delta/t \in [-2, 2]$ with $t = 1$, $L = 128$ and for various $\gamma =$ (a) 1×10^{-3} ; (b) 2×10^{-2} ; (c) 3×10^{-2} ; (d) 5×10^{-2} ; (e) 9×10^{-2} ; (f) 6.2×10^{-1} ; (g) 7.6×10^{-1} ; (h) 7.97×10^{-1} ; (i) 9.25×10^{-1} ; (j) 2; (k) 4.37.

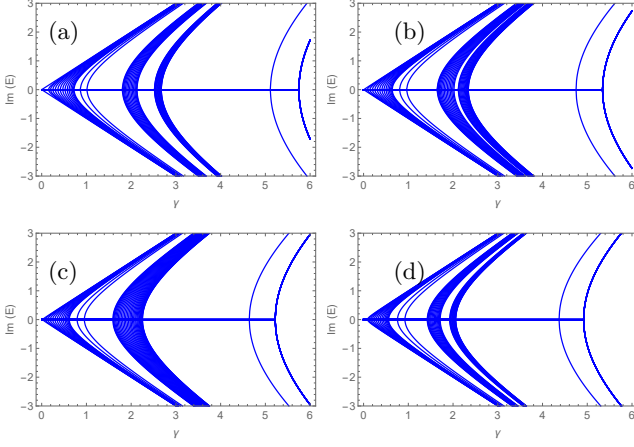


FIG. 7. Numerical spectra of the **imaginary part** of the eigenvalue under **OBC** with respect to γ with $t = 1$, $L = 128$ and $\Delta/t =$ (a) 3 (system in the TNP), (b) 2.7 (close to phase boundary in a part of the TNP), (c) 2.61 (at the phase boundary) and (d) 2.387 (system in the TTP). The inset shows the appropriate position of SPT BT point.

directions in the SSH chain gives rise to the localization of bulk states near the boundary along with topological end states and it can be understood as an outcome of the non-Hermitian skin effect of non-reciprocal lattice[31, 32]. Furthermore, the introduction of non-Hermitian parameter γ between site 1 and site 2 (off-diagonal non-Hermitian terms)[31] and between the same pair of sites (diagonal non-Hermitian terms) exhibit non-Hermitian skin effect leading to skewed profiles of the bulk states[33–35].

We mention here of a \mathbb{Z}_2 non-Hermitian skin effect (symmetry protected skin effect) of a spinful canonical system which respects time-reversal symmetry i.e., $TT^* = -1$ as studied by Okuma *et. al.*[30]. Their study reveals that a pair of skin modes (Kramers doublet) is localized at the two boundaries of the chain. Interestingly, the localization of end states above γ_{ep} for our periodically modulated non-Hermitian open chain however seems to be the localization of Kramers doublet.

Based on the above discussion, it is now apparent that the addition of non-Hermitian controlling parameter γ has no appreciable effect on the properties of the end, in-gap, and bulk states.

IV. SUMMARY AND CONCLUSIONS

In this paper, we have investigated the topological properties of the \mathcal{PT} symmetric periodically hopping modulated non-Hermitian SSH chain. We delve into accumulating the properties of the non-Hermitian end, in-gap, and bulk states. This work realizes the previously adopted connection between topological phases and SPT BT with more clarification. Our analysis shows that SPT BT is related to EP as well as \mathcal{PT} symmetric transition point. In the TNP regime, we noticed that the

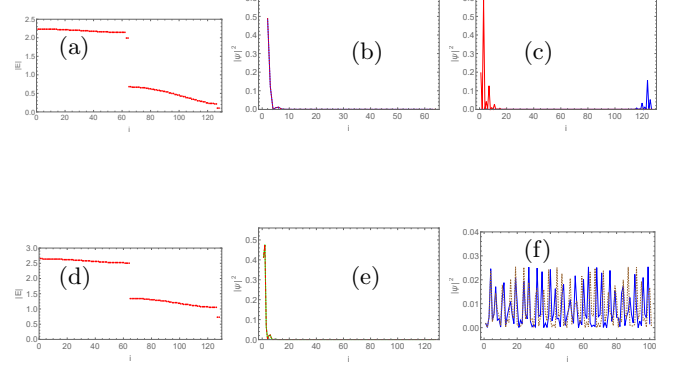


FIG. 8. Absolute value of energy eigenvalues and probability density (taking absolute values of amplitudes at lattice site i) of complex end states in the TNP for $\theta = \pi/2$ with $\Delta/t = 7.32 \times 10^{-1}$ (a)-(c). The same for the TTP with $\Delta/t = 1.56$ (d)-(e). (f) Profile of bulk states in the TNP with $\Delta/t = 7.32 \times 10^{-1}$.

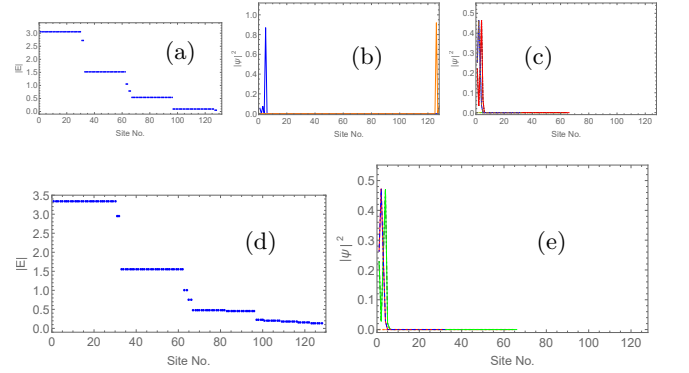


FIG. 9. Absolute value of energy eigenvalues and probability density (taking absolute values of amplitudes at lattice site i) of complex end states in the TNP for $\theta = \pi/4$ with $\Delta/t = 1$ (a)-(c). The same for the TTP with $\Delta/t = 1.2$ (d)-(e).

SPT BT occurs at EP which is close to the \mathcal{PT} symmetric transition point in a part of the TNP whereas deep into the TNP, one can notice only one SPT BP for all arbitrary nonzero γ values. In addition, in the TTP region, the considered model is consistent with Ref.[6] and shows a SPT BT at a γ_c , below which the model has only real eigenvalues and all the eigenvalues above γ_c becomes complex. This further justifies that there exists no such universal correlation between the topological properties and the SPT BT as studied in pioneer works[4, 6]. However, the \mathcal{PT} symmetry of the whole system is determined by visualizing the symmetry property of individual end states[5].

The summary of the results obtained is enlisted in Table II and III. The inclusion of the non-Hermiticity controlling parameter γ at the onsite term in a periodically

$\theta = \pi$					
System	TNP			TTP	
	ZES	In-gap states	Properties	ZES	In-gap states
Hermitian	Two zero energy states	-	Deep within the phase, this pair survive at single boundary however, they can survive at both the boundaries near QPT.	-	-
Non-Hermitian	One imaginary conjugated pair.	-	For $\gamma < \gamma_{ep}$ energies are real. Otherwise, ZES becomes imaginary conjugated, show peaks at both ends but with different amplitudes [Fig.3(c)-(d)]. Away from QPT, single peak observed at one end.	-	-

TABLE II. Comparative features of Hermitian and non-Hermitian system for $\theta = \pi$.

hopping modulated SSH chain associate the ZES with complex value for energy indicating dissipation in the system. Also, the nonzero energy eigenvalues of in-gap and bulk states for the Hermitian case now become complex when γ is turned on. In this respect the distinctive

localization nature of the end and in-gap states is also worth mentioning. Overall this distinctive and dissipative behavior of this system make its dynamics interesting and can be conveniently utilized in the field of quantum computations.

$\theta = \pi/2 (\pi/4)$						
System	TNP			TTP		
	ZES	In-gap states	Properties	ZES	In-gap states	Properties
Hermitian	Two (Two)	Two (Six)	Deep within the phase, the pair of ZES survive at a single end. Near QPT, they survive at both the boundaries. In-gap states peaks near single end.	-	Two (Six)	Same as in TNP.
Non-Hermitian	One imaginary conjugated pair (same)	One (three) pairs of purely real modes that become purely imaginary for large γ and close to $\Delta = 0$.	Only when $\gamma > \gamma_{ep}$, ZES becomes imaginary conjugated, show peaks at both ends but with different amplitudes [Fig.8(c)]. Away from QPT, single peak observed at one end. The pairs of in-gap states always show peaks at single ends [Fig.8(b)].	-	One complex pair (Three complex pair)	same as in TNP.

TABLE III. Comparative features of Hermitian and non-Hermitian system for $\theta = \pi/2 (\pi/4)$.

ACKNOWLEDGEMENTS

This work is financially supported by DST-SERB, Government of India via grant no. CRG/2022/002781.

- [1] R. Shankar, [Principles of Quantum Mechanics](#) (Springer, New York, 1994). [2] C. M. Bender and S. Boettcher, [Phys. Rev. Lett.](#) **80**, 5243 (1998); C. M. Bender, D. C. Brody, and H. F. Jones, [ibid.](#)

- 89**, 270401 (2002).
- [3] Simon Lieu, *Phys. Rev. B* **97**, 045106 (2018).
 - [4] Xiaohui Wang, Tingting Liu, Ye Xiong, and Peiqing Tong, *Phys. Rev. A* **92**, 012116 (2015).
 - [5] Marcel Klett, Holger Cartarius, Dennis Dast, Jörg Main, and Günter Wunner, *Phys. Rev. A* **95**, 053626 (2017).
 - [6] Baogang Zhu, Rong Lü, and Shu Chen, *Phys. Rev. A* **89**, 062102 (2014).
 - [7] Tian-Shu Deng and Wei Yi, *Phys. Rev. B* **100**, 035102 (2019).
 - [8] E. Sliotman *et. al.*, Topological Monomodes in non-Hermitian Systems, [arXiv:2304.05748v3 \[cond-mat.mes-hall\]](#).
 - [9] Felix Dangel, Marcel Wagner, Holger Cartarius, Jörg Main, and Günter Wunner, *Phys. Rev. A* **98**, 013628(2018).
 - [10] M. Martínez, A. Buendía, and J. Muga, [arXiv preprint, arXiv:1805.04968](#) (2018).
 - [11] A. F. Tzortzakakis *et. al.*, *Phys. Rev. A* **106**, 023513 (2022).
 - [12] K. G. Makris, R. El-Ganainy, D. N. Christodoulides, and Z. H. Musslimani, *Phys. Rev. Lett.* **100**, 103904 (2008).
 - [13] C. E. Rüter, K. G. Makris, R. El-Ganainy, D. N. Christodoulides, M. Segev, and D. Kip, *Nat. Phys.* **6**, 192 (2010).
 - [14] K. Esaki, M. Sato, K. Hasebe, and M. Kohmoto, *Phys. Rev. B* **84**, 205128 (2011).
 - [15] S. Mandal, S. Kar, [arXiv:2402.01236 \[cond-mat.str-el\]](#).
 - [16] S. Ryu and Y. Hatsugai, *Phys. Rev. Lett.* **89**, 077002 (2002).
 - [17] S. Weimann, M. Kremer, Y. Plotnik, Y. Lumer, S. Nolte, K. G. Makris, M. Segev, M. C. Rechtsman, and A. Szameit, *Nat. Mat.* **16**, 433438 (2017).
 - [18] Li-Jun Lang, You Wang, Hailong Wang, and Y. D. Chong, “Effects of non-Hermiticity on Su-Schrieffer-Heeger defect states”, *Phys. Rev. B* **98**, 094307 (2018).
 - [19] Tony E. Lee, *Phys. Rev. Lett.* **116**, 133903 (2016).
 - [20] H. Schomerus, *Opt. Lett.* **38**, 1912-1914 (2013).
 - [21] Y. C. Hu and T. L. Hughes, *Phys. Rev. B* **84**, 153101 (2011).
 - [22] The phase boundary should change while increasing non-Hermiticity strength γ as demonstrated in Fig.1.
 - [23] One can notice that the model has weak Δ (γ will also be very small) close to the transition point.
 - [24] L. Xiao *et. al.*, *Nature Physics* **13**, 1117 (2017).
 - [25] D. Cheng *et. al.*, *Phys. Rev. B* **105**, L201105 (2022).
 - [26] Z. Zhang *et. al.*, *Ann. Phys.* **533** 2000272 (2020).
 - [27] K. L. Zhang, P. Wang, G. Zhang, and Z. Song, “Simple harmonic oscillation in a non-Hermitian Su-Schrieffer-Heeger chain at the exceptional point”, *Phys. Rev. A* **98**, 022128 (2018).
 - [28] The matrix $Q(k)$ is Hermitian i.e., $Q(k)^\dagger = Q(k)$ and it follows the anticommutation relation $\{Q(k), \sigma_3\} = 0$.
 - [29] J. K. Asbóth, L. Oroszlány, and A. Pályi, “A Short Course on Topological Insulators”, *Springer International Publishing*, (2016).
 - [30] N. Okuma, K. Kawabata, K. Shiozaki, and M. Sato, Topological Origin of Non-Hermitian Skin Effects, *Phys. Rev. Lett.* **124**, 086801 (2020).
 - [31] Yan He and Chih-Chun Chien, *J. Phys.: Condens. Matter* **33** 085501 (2021).
 - [32] C. Yuce, Non-Hermitian anomalous skin effect, *Physics Letters A*, Volume 384, Issue 4, 2020.
 - [33] Yao S and Wang Z, *Phys. Rev. Lett.* **121** 086803 (2018).
 - [34] Martinez Alvarez V M, Barrios Vargas J E and Foa Torres L E F, *Phys. Rev. B* **97** 121401(R) (2018).
 - [35] Song F, Yao S and Wang Z, *Phys. Rev. Lett.* **123** 170401 (2019).